Journal of Materials & Environmental Sustainability Research (2022), 2(1): 39-52
p-ISSN: 2811-1338; e-ISSN: 2811-132X
DOI: https://doi.org/10.55455/jmesr.2022.003

Original Research Paper

Comparative AFM studies on the morphology of conducting polymers/DNA templated nanowires

Yahaya Mansur Ibrahim*

Chemistry Department, Sokoto State University, Sokoto, Nigeria
*Correspondence: ymansur64@gmail.com

Received: January 25, 2022; Revised: March 23, 2022; Accepted: April 3, 2022; Published: April 16, 2022

Handling Editor: Hooi Ling Lee

Abstract
Comparative morphological studies of three conductive polymers (polyimidazole (Plm), polyindole (Pln), and polypyrrole (Ppy)) templated with deoxyribonucleic (DNA) were carried out on silicon (Si)/mica substrate with the aim of finding more insight about the extent of mixing of the polymers with the DNA and the size of the nanowires formed. Atomic force microscope (AFM) height images of bare DNA on pre-treated substrates revealed a two-dimensional network structure with an average height of approximately 1.60 ± 0.01 nm; which is close to the double stranded DNA chain height. Plm/DNA exhibits globular and agglomerate nanostructures for the concentrated polymers, while the diluted form reveals a dispersed network with a diameter of 3 - 5 nm mostly. In Pln/DNA, the AFM images show dense networks of nanowires in their concentrated form, while the diluted samples displayed individual single wires with regular and smooth morphologies. Statistical analysis of the nanowires AFM heights revealed the dominance of wires with diameters in the range of 3 - 4 nm. The most common nanowire height range was 9 - 10 nm. Comparing the three polymer AFM studies, it can be said that polypyrrole has the highest nanowires range of 9 - 10 nm, then Plm/DNA (3 - 5 nm) and the least is Pln/DNA with 3 - 4 nm range. From the nanowire sizes and morphologies (uniform, smooth and continuous), it can be concluded that both polymers have good potentials for DNA templating and application in nanoelectronic devices as they can be aligned on nanoelectrodes for passage of electricity.

Keywords: Morphology; polymer; nanowires; sensing; DNA

DOI: 10.55455/jmesr.2022.003

1. Introduction

Conductive polymers (CPs) are polylink compounds having conventional organic polymers electronic properties and at the same time, retaining those similar to metals. Since the success in changing the electrical properties of some conductive polymers to exceptionally electrical conductivity, several conjugated polymers have been transformed from an insulator to a highly conductive state via halogenation (Narducci 2022; Park et al. 2021). Chain conformational changes, redox reactions, ion adsorption/desorption, volume/weight changes or charge transfer/screening are among the sensing mechanisms in conductive polymers. The above features, along with chemicals sensitivity, room temperature operation, and tunable charge transport properties, have launched conductive polymers as a major class of chemical transducers. Additionally, their synthetic routes are compatible with several functionalization schemes, including covalent bonding to the monomer, entrapment during synthesis, and surface chemistries, which can impart a high degree of selectivity and are conducive to several sensor modalities (Wang et al. 2021; Li et al. 2018).

DNA is an effective template for the conformation of nanowires (NWs) by wet chemical styles because it's available as extremely monodisperse samples with exceptional control over the length and it's chemically robust. It will retain its introductory structural integrity under the response conditions necessary to form conductive

polymers and metals in as much as high temperature or strong acid are not required (Mitchell and Olley 2018). Conductive polymers are attractive materials to template on DNA because together they form smooth, conductive nanowires (NWs) which provide access to a wide range of chemical functionality for subsequent applications. Whilst inorganic NWs may be functionalised using methods originally developed for bulk substrates, the polymer NWs can be functionalised simply by derivatisation of the monomer and the density of functional groups are adjusted by copolymerisation. (Mohamed et al. 2012; Wei et al. 2019).

AFM is a microscope used for the characterization of various processes at the nanoscale that involve investigations of quantitative single molecules (Maver et al. 2016) It is an exceptional tool for studying the application of temporal shifts in the morphology of polymers (Magonov 2008). As an important tool, AFM is commonly used in the field of polymer crystallisation (Nguyen-Tri et al. 2020). It does not require sample staining or metal coating. Hence, it is straightforward to prepare the specimen for imaging (Odijk and Vanden 2018).

Although many studies about the morphology of polymer/DNA templated nanowires using AFM have been conducted and there are numerous publications dealing with the subject, but comparative AFM height image studies on the morphology of different conducting Polymers/DNA templated nanowires can give more insight about the extent of mixing of the polymers with the DNA, size of the nanowires formed and their possible applications in nanoelectronics devices, which is the aim of our research.

2. Materials and Methods

Exactly, 5 μL of the mixture of conductive polymer and DNA samples, which were obtained from Biolab, UK, prepared as explained in previous reports (Yahaya, 2020a; Yahaya, 2020b) were dropped-cast on a cleaned silicon substrate. The samples were dried in an airflow cabinet for 12 hours prior to AFM analysis. The MultiMode 8 Scanning Probe Microscope was used to obtain AFM height images. The equipment was operated in tapping mode using silicon doped cantilevers, resonant frequency range of 230 to 410 kHz, with force constant ranging from 20 to 80 Nm^{-1}. The sensitivity of the cantilevers was determined with the assumption that there was no deformation of the tip and sample. An isolation table was used to minimise noise from vibration.

3. Results and Discussion

DNA-templated deposits of conducting polymer nanowires display a lower and more constant width than metal nanowires, presumably owing to the fairly slow reaction rate and thereby good controllability of polymerization. The tapping mode AFM height images of water-diluted DNA on Silicon substrates are displayed in Figure 1. A lattice of DNA bundles and some Rope-like structures can be seen in the Figure 1. The result is similar to other reported works on the formation of well-defined DNA structures on silicon substrates. When deposited using divalent cations, upon drying, shortening of DNA molecules were observed and were consistent in magnitude with a partial B- to A-form conformational transition (Konrad et al. 2021; Bose and Tuân 2017). Despite the fact that concentration and kinds of DNA and counterions present in solutions, network treatment after formation and surface properties were among the factors that were assumed to be responsible for network formation, even though it is not a conclusive idea. Overlapping of circles where divalent charged positive ions serve as salt bridges between DNA, surface and between chains were suggested as mechanisms for network formation in DNA. Triple strand splitting and double strand DNA organisation is another similar mechanism for network formation by overcrossing of linear DNA chains (Yamaguchi et al. 2021; Marchetti and Guo 2020).

In Figure 2, an AFM image of bare DNA molecules adsorbed on mica surfaces were revealed. In this work, bare DNA refers to the DNA prior to templating of conductive polymers. From the figure, it can be seen that the mica substrate was enveloped by a two-dimensional network of DNA. The fibre heights of the network structures were evaluated using height measurements of the DNA molecules acquired using the bearing function of the image analysis software (Bruker: NanoScope Analysis version 1.5) to calculate the height of the strands in 3 different spheres and it was found to be approximately 1.60 ± 0.01 nm, which is very close to the double stranded DNA chain height, that was found to be around 1.5 to 2.0 nm (Cervantes and Medina 2014; Ganguli et al. 2004). Just like in our work, single stranded DNA molecules on mica have compact structures, while on another substrate, like modified highly oriented pyrolytic graphite (HOPG), acquires a conformation without secondary structures,

based on which Adamcik et al. (2006) concluded that the intramolecular base-pairing was eliminated by restriction of ssDNA under standard conditions on modified HOPG.

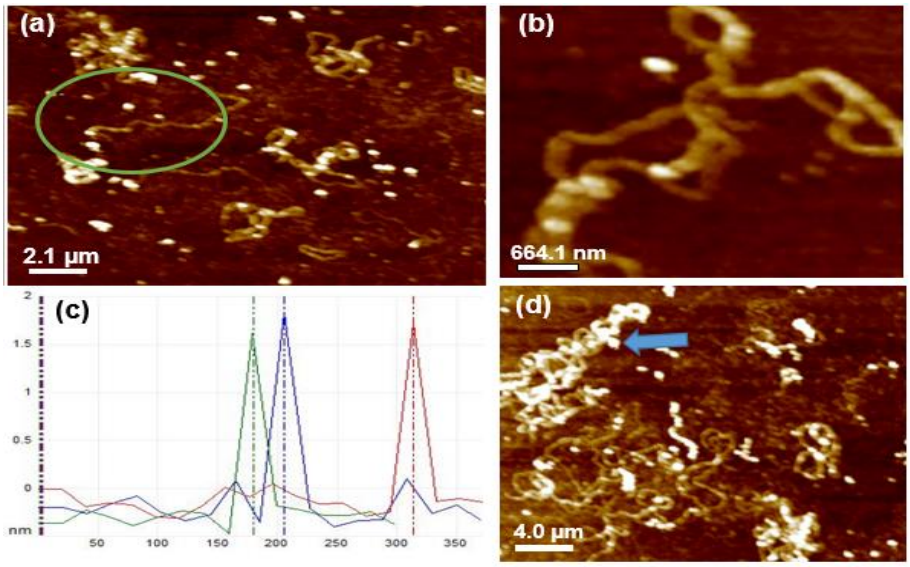

Figure 1: Bare DNA AFM images and height profile: (a) network of DNA bundles with some rope like structures being formed (b) zoomed image of the rope like molecule (c) DNA height profile (d) unfolding coil like network of the bare DNA molecule

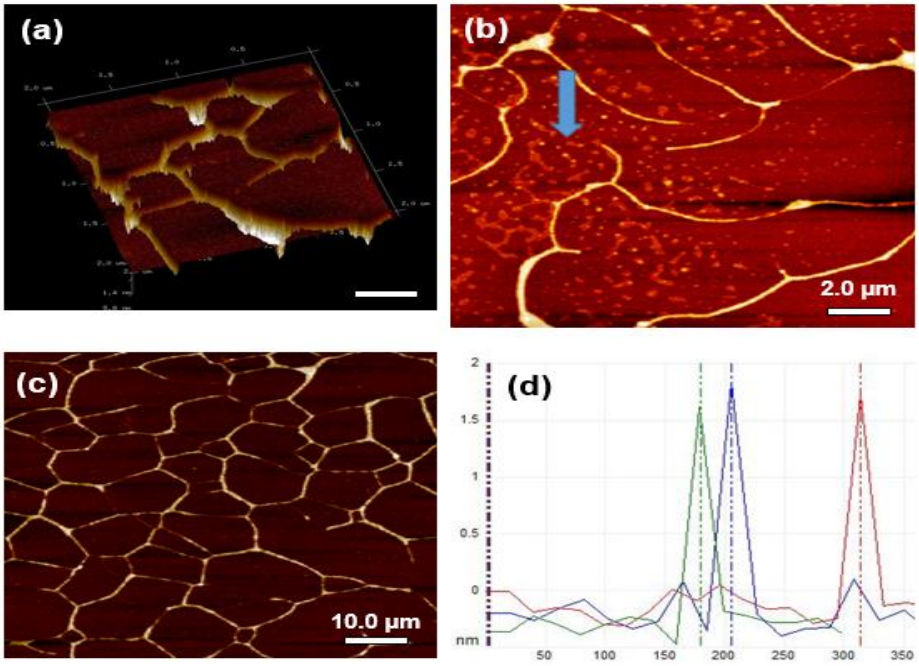

Figure 2: Height AFM images of water diluted bare DNA on mica substrate: (a) 3D image of λ-DNA (b) AFM image showing the individual ropes (c) bare DNA molecules adsorbed on mica surface and d) AFM height profile

In our work, it was assumed that when mica Substrates are immersed in DNA solution, molecules are deposited on the mica. surfaces and network structures are formed due to entanglement and aggregation of the DNA chains and the added MgCl2 solution makes mica positive and easily adsorb the nanowire film. The attractive forces (van der Waals, intermolecular forces, electrostatic forces and so on) of all kinds between DNA and mica were

likely to be responsible for the morphological transformation of DNA molecules (Gosika et al. 2020; Yamada and Kobayashi 2019). Andreyuk (2006), found similar results like ours when they visualised net-like structures formed by several bases pair long DNA molecules that were transferred from solution to mica surface using contact and tapping mode AFM. They also investigated the influence of DNA end structure and found single strand ends increase the efficiency of the network formation and proposed that network junctions may occur at distortion sites of the DNA chain.

In Figure 3, the AFM images and profile heights of Plm/DNA nanostructures are delineated. The images exhibit a spherical shape, agglomerate and dense rope-like networks for the diluted and undiluted nanomaterials respectively. The result obtained, as shown in figure 3, is in agreement with Al-Hinai et al. (2016) findings that AFM images of Plm/DNA hybrids can prove the formation of polyimidazole beside the DNA strands. Their work clearly distinguished Plm/DNA nanowires from bare DNA using their AFM height measurements by comparing the heights of the wires appearing in the AFM image which are aligned after approximately 2 hours of incubation, they confirmed that the polymer begins to coat DNA, but at the same time there is plenty of uncoated DNA strands and a lot of agglomerated material of the DNA template. This agglomeration is believed to be due to either free polymer or the presence of residuals of buffer salts or both (Cervantes and Medina 2014). Likewise, condensation of DNA strands due to shielding of charges on the phosphate groups of the DNA by the action of metal ions can be another reason (Moreno-Herrero et al. 2003).

Figure 4 further elucidates the rope-like network of the Plm/DNA nanowires, which demonstrates the suggestion that the DNA/polymer composite in which the charge on the DNA is atone by the cationic polymer forming rope-like structures (Nagarajan et al. 2008) The importance of tuning the incubation time with monomer unit and DNA concentrations to find an agreeable balance between non-specific depositions, rope formation and nanowire coverage have been proved by this result as was the case in similar studies elsewhere. It was suggested that when high concentration of monomer, DNA and/or extended incubation times are utilised, polymerisation is no longer directed along the duplex in a linear fashion but instead DNA/polymer simply aggregates in an uncontrolled manner, identical to condensation of DNA by multivalent cations and cationic polymers, giving rise to a greater degree of height variation in addition to difficulties during nanowire deposition (Watson et al. 2012).

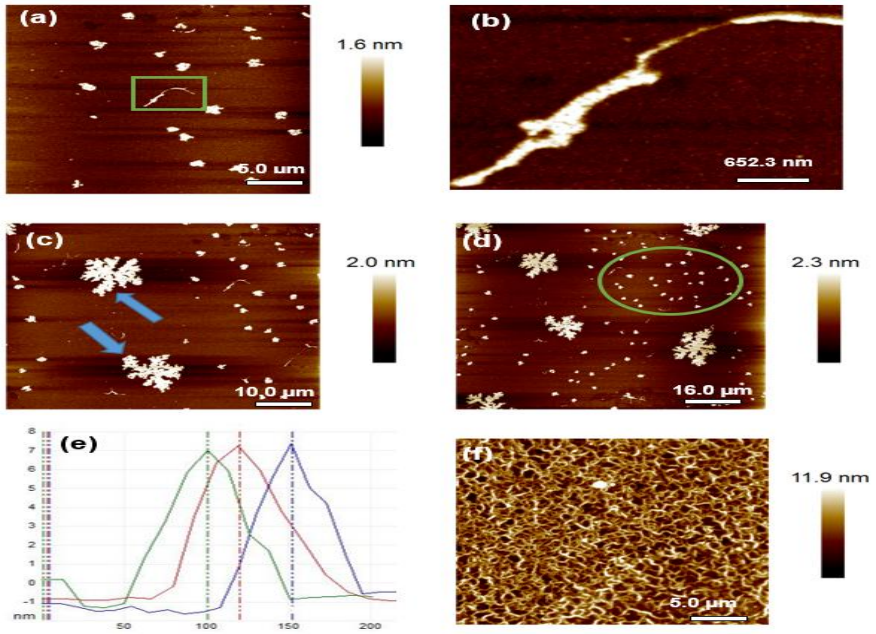

Figure 3: AFM images of Plm/DNA on Silicon substrate after 24 hours incubation (a) Spherical shaped images (b) enlarge strand bound by the CP (c) agglomerate disperse structures (d) small spherical shape nanostructures (e) AFM height profile] (f) Dense rope like network of concentrated mixture.

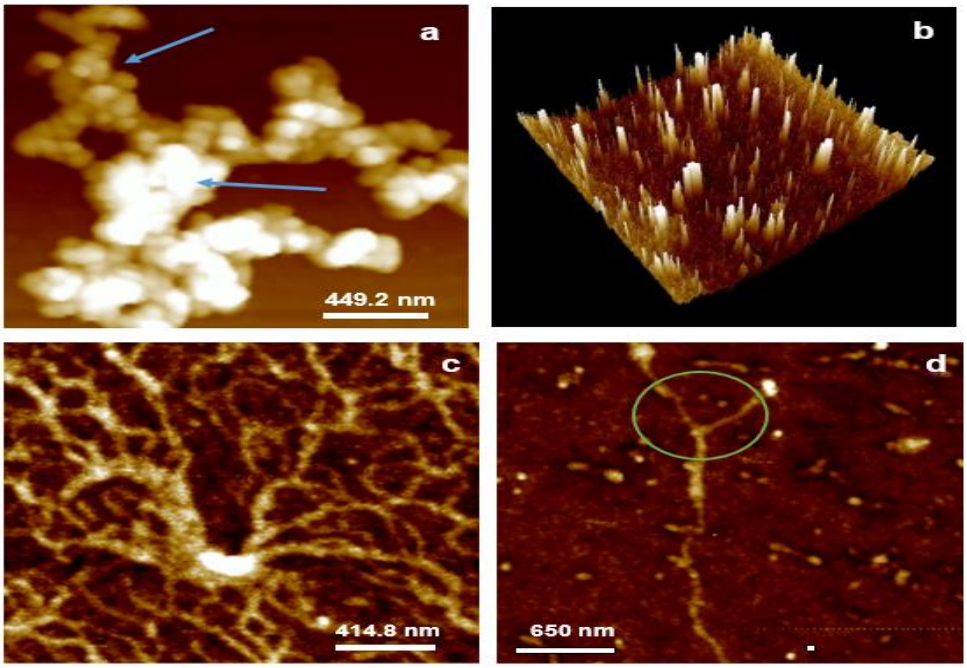

Figure 4: Plm/DNA nanostructures AFM height images: a, b and c show a network of white polymer materials along the DNA and (d) nanowires strand with polymer coating

In previous studies (Yahaya 2020a, b), numerical analysis of 150 Plm/DNA nanowires with more than one hour incubation period revealed 3 - 4 nm as the modal diameter. Few structures with diameters greater than 13 nm were also observed. Watson et al. (2013) attributed these larger structures to the wrapping of the CPs/DNA structures into larger rope-like assemblies. They assumed that the formation of polymer on DNA takes place initially through low density binding spherical conducting polymer particles on the duplex DNA. The size and density of these polymer particles on the DNA increases as the reaction proceeds, leading to a beads-on-string appearance. The loading of DNA with CP is increased with increasing reaction time and the polymer begins to undergo change in shape, becoming elongated along the DNA axis and amalgamate into one another, finally producing polymer nanowires of highly smooth and regular structure.

To probe the results of incubation time on topography of nanowires, Pln/DNA nanomaterials with different polymerisation time were drop cast on SiO2 surface and AFM height images were captured and shown in Figures 5 and 6 for short and long time incubation respectively, the differences observed are that network/bundles of polymer materials were observed for a short time while with a long synthesis time, thick polymer films were seen. This is similar to previous observations elsewhere (Wadatkar and Waghuley 2019; Meers et al. 2016), it was believed that hydrophobic surfaces favoured the observation of individual nanowires, and hydrophilic surfaces adsorbed high density nanowires (Soler et al. 2019).

Some researchers observed changes in morphology of polypyrrole nanostructures upon standing in the polymerisation solution, individual nanowires were found to combine together to form ropes and adjusting the hydrophobicity of the substrate leads to an increase in the extent of silanization (Stejskal & Prokeš, 2020). In another study, Hassanien et al. (2010) found that the distinction between the Ppy/DNA and PIn/DNA systems is that the latter structure is smoother and their thickness is uniform along the length of the nanowire after a reaction time of 24 h. In their work, AFM measurements were carried out on samples of Ppy/DNA structures, aligned upon silicon substrate after different reaction times (5, 10 and 30 minutes and 1, 4 and 24 hours). AFM imaging of the sample isolated after a reaction time of 5 minutes shows evidence for the formation of conductive polymers as approximately spherical particles bound to DNA strands at random points along the duplex structures. They are bound to the DNA at low density with free DNA clearly seen between adjacent particles. A range of particle sizes, from 18 - 28 nm, is observed. After increasing the reaction time to 10 minutes, the density and size of the polymer particles on DNA are noticeably increased. In this case, the polymer particles have a density ~ 6

particles/micron, and diameters ranging from 13 - 47 nm. At this incubation time, however, although the majority of the polymer particles attached to DNA still have their initial spherical shape, one can also see some which have become extended along the DNA axis, which is similar to our result.

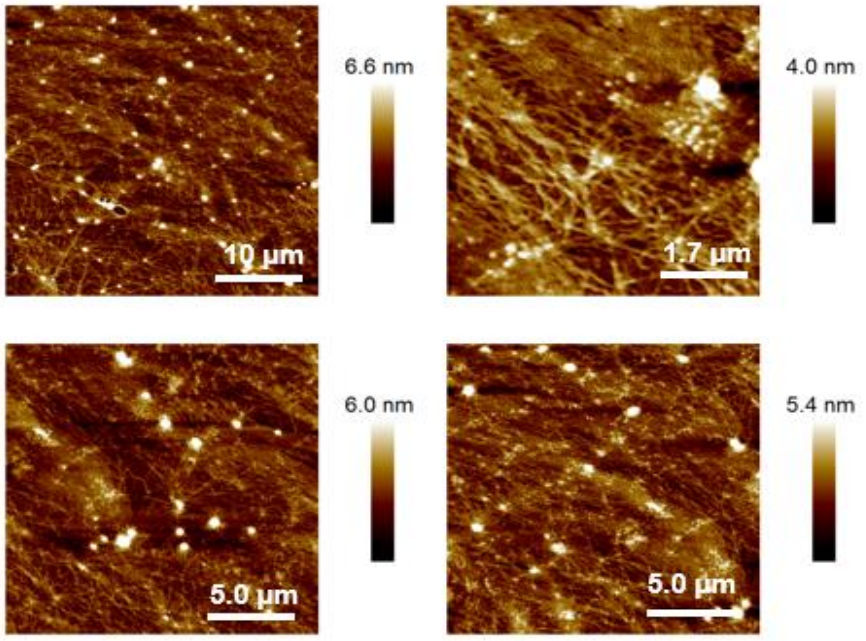

Figure 5: AFM height images of high concentration Pln/DNA on Si/SiO_2 surface with short polymerisation time.

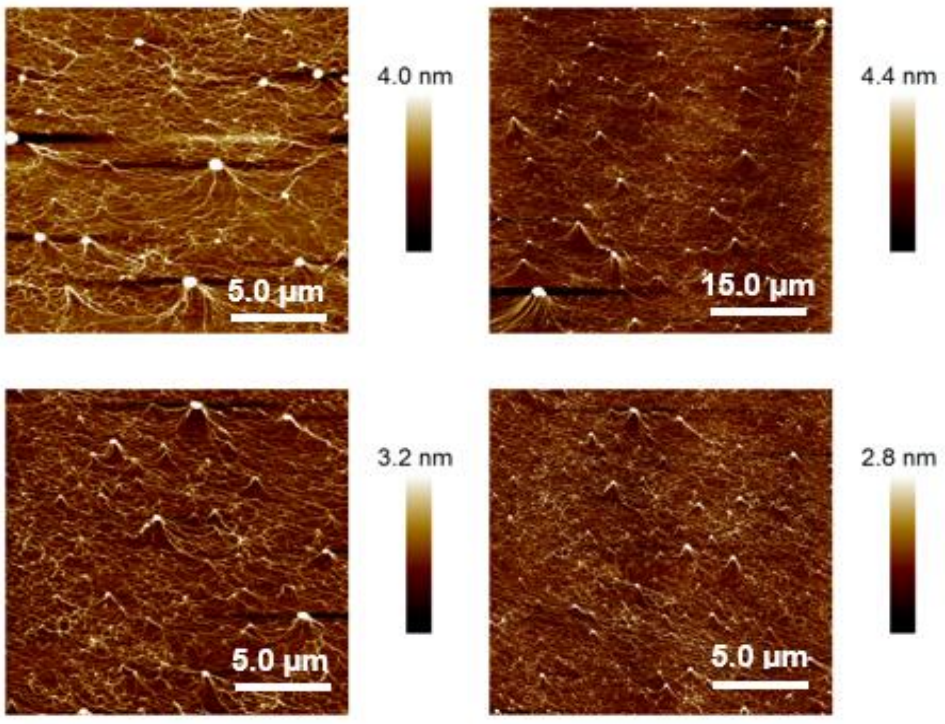

Figure 6: AFM height images of concentrated Pln/DNA on Si/SiO_2 surface with long synthesis time.

When the Polyindole/DNA nanomaterials were imaged on silicon and mica (Figures 7 and 8, respectively), nanostructures were clearly observed which exhibited a regular and smooth shape with complete and continuous coverage of the duplex DNA by the polymer material. The nanostructures have shown relatively similar morphologies to other polymer nanowires prepared using DNA as a template (Pruneanu et al. 2008; Park et al. 2020).

Despite the fact that the complete, regular and smooth appearance of the Polyindole DNA templated nanowires was attained in a shorter time in contrast with the earlier mentioned examples of polymer nanomaterials, a huge number of agglomerated materials were also observed and believed to be due to the effect of their local hydrophobicity/hydrophilicity relative to the supporting surface (Peil et al. 2020).

The dominance of 3 - 4 nm diameter range nanowires was revealed by numerical analysis of 150 Pln/DNA nanowires in our previous work (Yahaya 2020b). Larger structures were also recorded indicating the prolongation of the polymerisation reaction after the nanowire formation was further revealed by the presence of nanowires with diameters greater than 13 nm.

Figure 9 reveals the PPy/DNA nanowires AFM height images, that shows different morphologies with materials indicating both a small number of bare DNA strands, (a-b) indicating that not all the DNA molecules were involved in templating, well aligned polymeric nanomaterials with regular coverage extended across the substrate and high density PPy/DNA films. In image (c) the height image shows a granular morphology, consisting of a linear assembly of nanomaterials densely arranged together along the DNA.

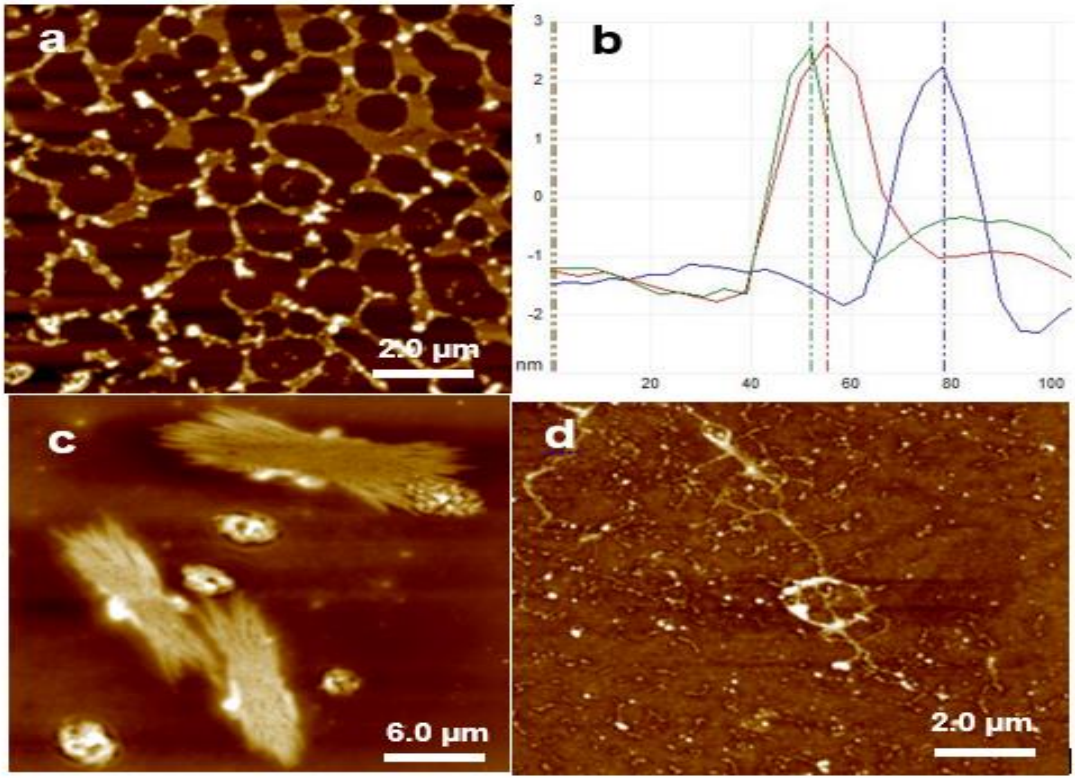

Figure 7: DNA templated polyinidole AFM images and profile heights: (a) multilateral network of Pln/DNA films (b) Profile height of the aligned nanowires (c) thick nanomaterials film (d) capillaceous shaped nanomaterials

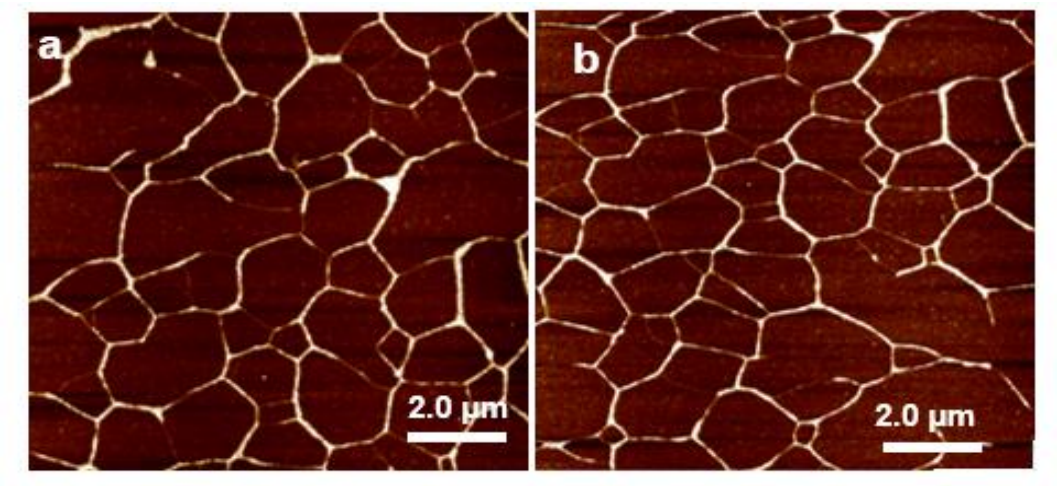

Figure 8: Pln/DNA AFM height images absorbed on mica surface, showing the hexagonal surface covered by the DNA-templated indole polymer.

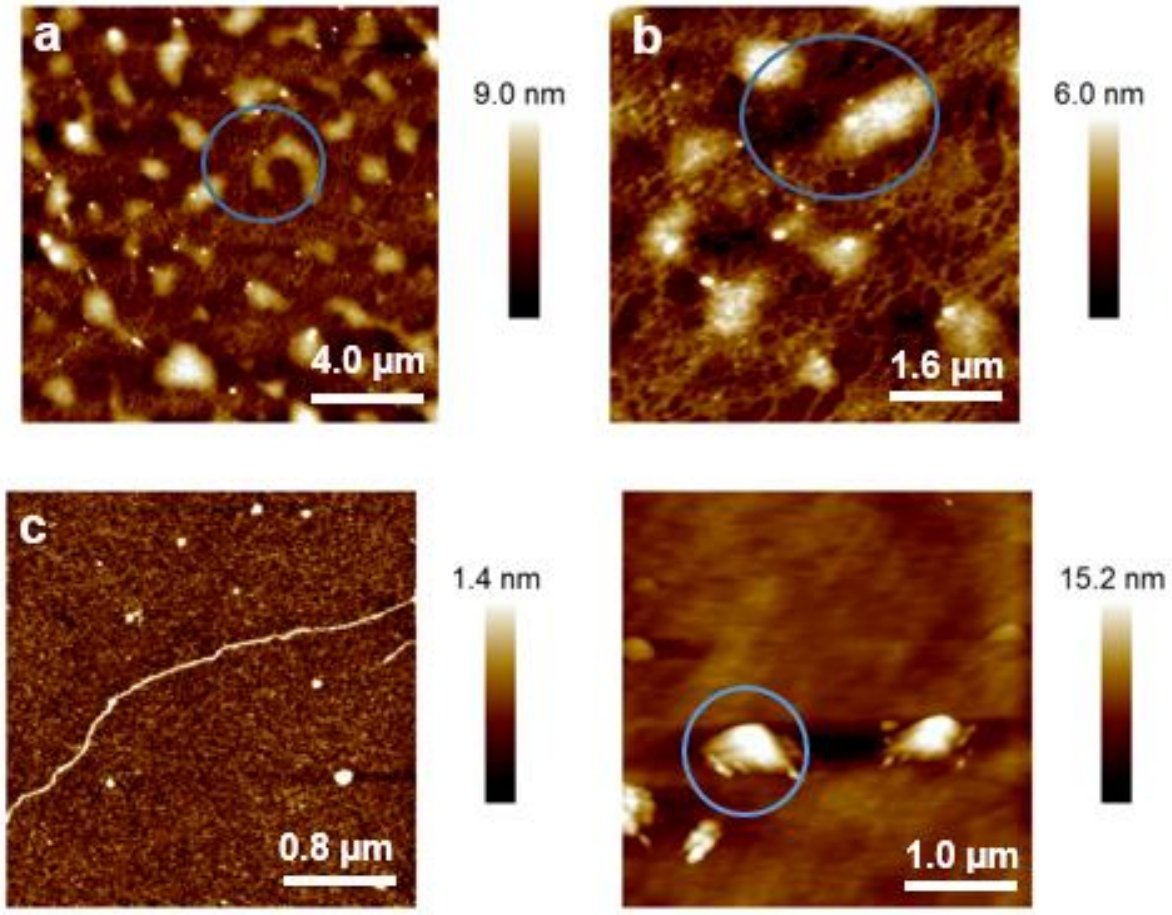

Figure 9: AFM images of PPy/DNA nanowires.: (a-b) PPy/DNA nanowires film's image showing (blue cycles) the polymer materials incorporating/ bounding to the DNA material(c) well aligned, polymeric nanomaterials with regular coverage extended across the substrate (d) nanostructures films.

Our results on pyrrole polymer, are similar to other work on the same polymer and have the same interpretation, for instance, Mao et al. (2016) explained in their studies of polypyrrole film diffusion through the self-affine surface, that fractal dimensions calculated by electrochemical methods represent more chaotic and complex behaviour for the polypyrrole film than fractal dimension obtained by AFM image, because some parts of porous media in the surface is not accessible to imaging devices just lie in our study. In another work, Marandi et al. (2010), found that over prolonged time of incubation, a self-assembly process occurs in which DNA templated conductive polymers nanowires to form ring-like structures which they refer to as nanoropes, by carefully analysing the AFM images they believed that the assembly process that form the rope-like structures consists of individual nanowire twisted around each other as in Figure 12b. They showed that silanization can be used to control the density of the nanoropes on silicon dioxide which allows for connecting them to a two terminal electrical device that can measure their electrical properties.

In Figure 10 are shown average AFM images and profile height of PPy/DNA nanomaterials. From the figure it is shown that (a-b) the substrate was covered by a two-dimensional meshwork of PPy/DNA, in (c) individual nanowires (green square) and an AFM height profile (d) indicating the uniform height of the PPy/DNA nanowires. These results may be due to the extent of polymerisation and level of mixing between the polymer and DNA. Moonet al. (2010), found that images from different aminopropyl silatrane treatment times and using the vortex process clearly showed the effect on the synthesis of individual and continuous polypyrrole nanowires. The nanowires at various polymer concentrations had similar heights while for the higher concentration a lot of residues were observed, just like in our work.

From a more elaborate statistical analysis of the PPy/DNA AFM height as shown in figure 11, the most common height was 9 - 10 nm range, which can be attributed to the standing time, that increases the thickness of the nanowires as the cluster process is gradual and continues for days, producing even thicker ropes (Chee et al. 2014; Sharifi-Viand et al. 2015).

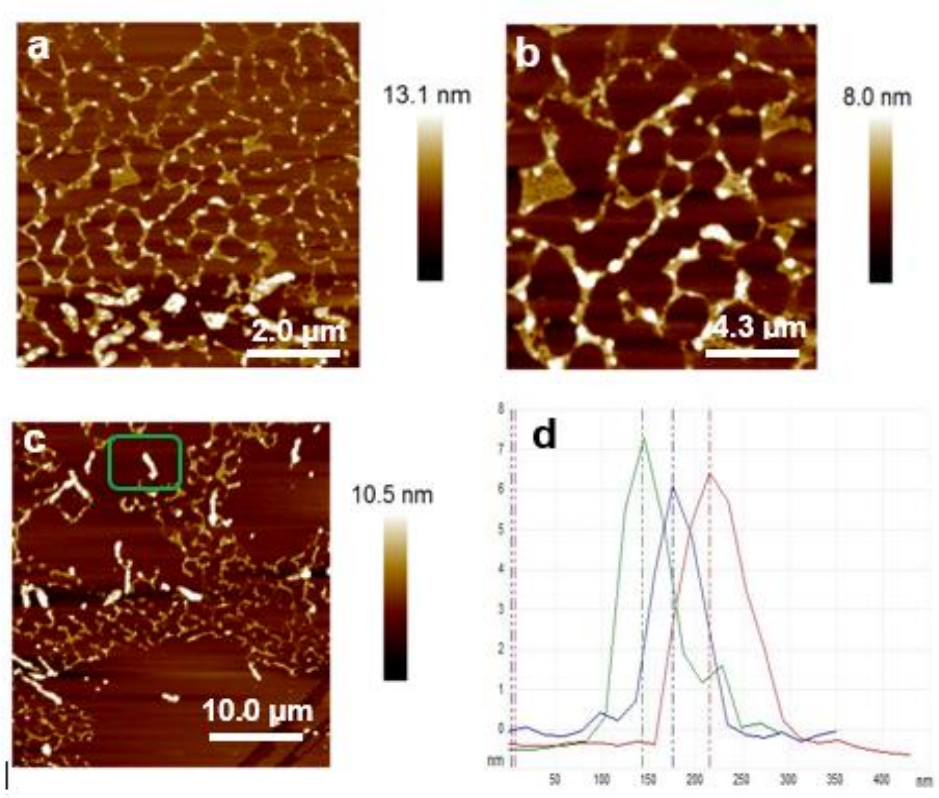

Figure 10: PPy/DNA AFM height image: (a–b) hexagonal/mesh like structures (c) individual PPy/DNA nanowires (green square) spread across the surface (d) height profile indicating the uniform height across the nanowires' length

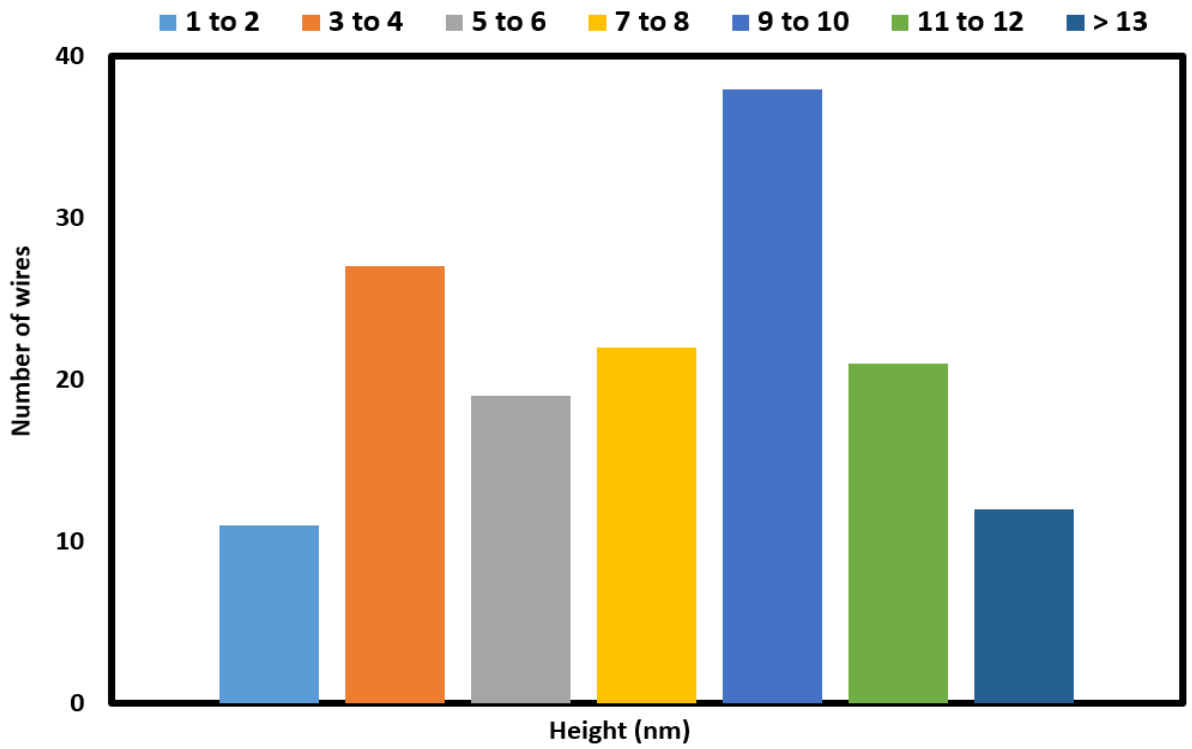

Figure 11: Bar chat revealing the heights of 150 PPy/DNA nanowires

Mechanism of Polymer DNA Templating

According to some researchers, nanowire formation by the growth mechanism of supramolecular structure method relies on the complementarity of the conductive polymer chains which are initially formed as short cationic oligomers, bind to the DNA through supramolecular interactions, like electrostatics plus additional noncovalent bonding, possibly in a manner analogous to small groove binding drug molecules. This then influences the growth of further polymers along the double-helix axis (Hogan 2018).

The mechanism may be considered to pass through several, rather structurally distinct forms and to involve a dramatic reorganisation of the conductive polymer strands over an exceptionally large, micrometre, length scale once bound to the DNA duplex. In the synthesis and immobilisation of bulk polypyrrole (PPy) films on DNA-modified silicon electrodes, for example (Fig. 12), the immobilisation arises from electrostatic interaction between the cationic, oxidised PPy and the polyanionic DNA. It was reasoned that, because pyrrole oligomers formed during the initial stages of oxidative polymerisation exhibit DNA-binding motifs, the formation of individual DNA/PPy hybrid strands should also be possible through supramolecular interactions.

The characteristics of the mechanism of DNA-templating are of fundamental interest, but also have significance for the major proposed applications of templated NWs as interconnects in electronic devices and as transducing elements in chemical sensors. In the case of interconnects, it is clearly desirable for the NWs to be uniform and continuous to attain the maximum possible conductivity, while in sensing, where the signal is typically a fractional change in conductivity upon exposure to the analyte, it may be more important for them to have a high surface: volume ratio to maximise the sensitivity and therefore a uniform, smooth morphology is not necessarily optimal. From our results, all the polymer nanowires have both uniform, continuous and smooth morphologies. Therefore, can be used as interconnects in electronic devices and as transducing elements in chemical sensors (Watson et al. 2014).

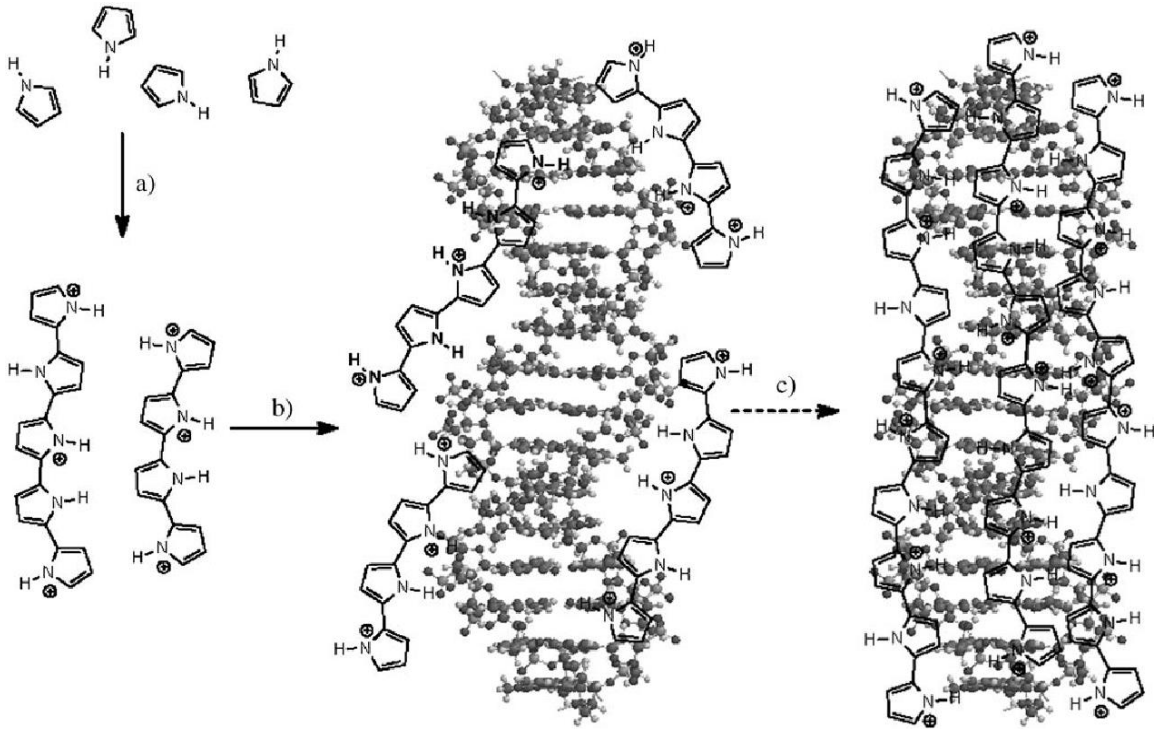

Figure 12.: Proposed mechanism of self-assembly of DNA-Polypyrrole nanowires. a) Oxidation of pyrrole monomer with $FeCl_3$, b) association of oligomers on DNA through supramolecular interactions, c) polymer growth on DNA template (Dong et al., 2007). Reproduced with permission from John Wiley & Sons.

4. Conclusion

AFM images of free DNA on pre-treated silicon substrates reveal a two-dimensional network of DNA structures with an average height of approximately 1.60 ± 0.01 nm, which is close to a double stranded DNA chain height of 1.5 – 2.0 nm. Similar behaviour was observed when the bare DNA images were acquired on mica substrate. Plm/DNA exhibits globular and agglomerate nanostructures for the concentrated polymers, while the diluted form reveals a dispersed network of the nanomaterials with a diameter of 3 - 5 nm mostly. In Pn/DNA materials imaged on mica and silicon substrate, where pretreatment modifies the surfaces to a hydrophobic form that reduces surface interactions with the hydrophilic nanowires, the AFM images show dense networks of nanowires in their concentrated form while the diluted nanowires displayed individual single wires with regular and smooth morphologies. Statistical analysis of the nanowire AFM heights indicated the predominance of 3 - 4 nm diameter nanowires. Polypyrrole DNA-templated nanomaterials on silicon and mica substrates show different morphologies in their AFM height images indicating both small numbers of bare DNA strands (because not all the DNA was involved in the templating of the polypyrrole); well aligned polymeric nanomaterials with regular coverage that extended across the substrate and high density PPy/DNA films (from the concentrated nanomaterials. The most common nanowire height range was 9 - 10 nm. Comparing the three polymer AFM studies, it can be said that all the three polymers revealed similar images under AFM, which is not surprising as both polymers are conjugated and have similar polymerisation mechanisms and the same mixing behaviour with the DNA template. Polypyrrole has the highest nanowire range of 9 - 10 nm, then Plm/DNA (3 - 5 nm) and the least is Pln/DNA with 3 - 4 nm range. The difference can be attributed to the rate of polymerisation of the different polymers, that results in their having different morphologies. From the nanowire sizes and morphologies (uniform, smooth and continuous), it can be said that all the three polymers have potentials for application as interconnects in electronic devices and as transducing elements in chemical sensors as they can be aligned on nanoelectrodes for passage of electricity.

Conflict of interests
None declared.

References

Adamcik, J., Klinov, D., Witz, G., Sekatskii, S. & Dietler, G. (2006). Observation of single-stranded DNA on mica and highly oriented pyrolytic graphite by atomic force microscopy. *FEBS Letters*, 580(24), 5671-5675. doi: 10.1016/j.febslet.2006.09.017

Al-Hinai, M., Hassanien, R., Watson, S., Wright, N., Houlton, A. & Horrocks, B. (2016). Metal-conductive polymer hybrid nanostructures: preparation and electrical properties of palladium–polyimidazole nanowires. *Nanotechnology*, 27(9), 095704. doi: 10.1088/0957-4484/27/9/095704

Andreyuk, D. (2006). NanoLaboratory concept: a platform combining advanced scanning probe microscopy and non-scanning probe microscopy methods. *Journal of Scanning Probe Microscopy*, 1(1), 51-54. doi: 10.1166/jspm.2006.005

Bose, K. & Tuân Phan, A. (2017). AFM imaging of DNA G-wires in solution. *Biophysical Journal*, 112(3), 587A. doi: https://doi.org/10.1016/j.bpj.2016.11.3161

Cervantes, N. & Medina, B. (2014). Robust deposition of lambda DNA on mica for imaging by AFM in air. *Scanning*, 36(6), 561-569. doi: 10.1002/sca.21155

Chee, W., Lim, H. & Huang, N. (2014). Electrochemical properties of free-standing polypyrrole/graphene oxide/zinc oxide flexible supercapacitor. *International Journal of Energy Research*, 39(1), 111-119. doi: 10.1002/er.3225

Dong, L., Hollis, T., Fishwick, S., Connolly, B., Wright, N., Horrocks, B. & Houlton, A. (2007). Synthesis, manipulation and conductivity of supramolecular polymer nanowires. *Chemistry - A European Journal*, 13(3), 822-828. https://doi.org/10.1002/chem.200601320

Ganguli, M., Babu, J. & Maiti, S. (2004). Complex formation between cationically modified gold nanoparticles and DNA: an atomic force microscopic study. *Langmuir*, 20(13), 5165-5170. doi: 10.1021/la036049a

Gosika, M., Mandal, T. & Maiti, P. (2020). Modulating interdendrimer interactions through surface adsorption. *Langmuir*, 36(20), 5492-5501. doi: 10.1021/acs.langmuir.0c00208

Hassanien, R., Al-Hinai, M., Farha Al-Said, S., Little, R., Šiller, L., Wright, N., Houlton, A. & Horrocks, B. R. (2010). Preparation and characterization of conductive and photoluminescent DNA-templated polyindole nanowires. *ACS Nano*, 4(4), 2149-2159. doi: 10.1021/nn9014533

Hogan, M. (2018). Templating life: DNA as nature's hard drive. *Public*, 29(57), 145-153. doi: https://doi.org/10.1386/public.29.57.145_1

Konrad, S., Vanderlinden, W. & Lipfert, J. (2021). A high-throughput pipeline to determine DNA and nucleosome conformations by AFM imaging. *BIO-PROTOCOL*, 11(19). doi: https://doi.org/10.21769/bioprotoc.4180

Li, F., Kaiser, M., Ma, J., Guo, Z., Liu, H. & Wang, J. (2018). Free-standing sulphur-polypyrrole cathode in conjunction with a polypyrrole-coated separator for flexible Li-S batteries. *Energy Storage Materials*, 13, 312-322. doi: 10.1016/j.ensm.2018.02.007

Magonov, S. & Whangbo, M.-H. (2008). *Surface Analysis with STM and AFM: Experimental and Theoretical Aspects of Image Analysis*. John Wiley & Sons. 335p. doi: 10.1002/9783527615117

Mao, J. & Zhang, Z. (2016). Conductive poly(pyrrole-co-(1-(2-carboxyethyl)pyrrole)) core-shell particles: Synthesis, characterization, and optimization. *Polymer*, 105, 113-123. doi: 10.1016/j.polymer.2016.10.022

Marandi, M., Kallip, S., Sammelselg, V. & Tamm, J. (2010). AFM study of the adsorption of pyrrole and formation of the polypyrrole film on gold surface. *Electrochemistry Communications*, 12(6), 854-858. doi: 10.1016/j.elecom.2010.04.005

Marchetti, A. & Guo, H. (2020). New insights on molecular mechanism of hepatitis B virus covalently closed circular DNA formation. *Cells*, 9(11), 2430. doi: 10.3390/cells9112430

Maver, U., Velnar, T., Gaberšček, M., Planinšek, O. & Finšgar, M. (2016). Recent progressive use of atomic force microscopy in biomedical applications. *TrAC Trends in Analytical Chemistry*, 80, 96-111. doi: 10.1016/j.trac.2016.03.014

Meers, C., Keskin, H. & Storici, F. (2016). DNA repair by RNA: Templated, or not templated, that is the question. *DNA Repair*, 44, 17-21. doi: https://doi.org/10.1016/j.dnarep.2016.05.002

Mitchell, G. & Olley, R. (2018). Orthogonal templating control of the crystallisation of poly(ε-caprolactone). *Polymers*, 10(3), 300. doi: https://doi.org/10.3390/polym10030300

Mohamed, H., Watson, S., Horrocks, B. & Houlton, A. (2012). Magnetic and conductive magnetite nanowires by DNA-templating. *Nanoscale*, 4(19), 5936. doi: https://doi.org/10.1039/c2nr31559a

Moon, H., Kim, H., Kim, N. & Roh, Y. (2010). Fabrication of highly uniform conductive polypyrrole nanowires with DNA templates. *Journal of Nanoscience and Nanotechnology*, 10(5), 3180-3184. doi: 10.1166/jnn.2010.2246

Moreno-Herrero, F., Colchero, J. & Baró, A. (2003). DNA height in scanning force microscopy. *Ultramicroscopy*, 96(2), 167-174. doi: 10.1016/s0304-3991(03)00004-4

Nagarajan, S., Kumar, J., Bruno, F., Samuelson, L. & Nagarajan, R. (2008). Biocatalytically synthesised poly(3,4-ethylenedioxythiophene). *Macromolecules*, 41(9), 3049-3052. doi: 10.1021/ma0717845

Narducci, R. (2022). Ionic conductive polymers for electrochemical devices. *Polymers*, 14(2), 246. doi: https://doi.org/10.3390/polym14020246

Nguyen-Tri, P., Ghassemi, P., Carriere, P., Nanda, S., Assadi, A. & Nguyen, D. (2020). Recent applications of advanced atomic force microscopy in polymer science: a review. *Polymers*, 12(5), 1142. doi: 10.3390/polym12051142

Odijk, M. & van den Berg, A. (2018). Nanoscale electrochemical sensing and processing in microreactors. *Annual Review of Analytical Chemistry*, 11(1), 421-440. doi: 10.1146/annurev-anchem-061417-125642

Park, D., Ju, H. & Kim, J. (2020). Effect of $SrTiO_3$ Nanoparticles in conductive polymer on thermoelectric performance for efficient thermoelectrics. *Polymers*, 12(4), 777. doi: 10.3390/polym12040777

Park, D., Kim, M. & Kim, J. (2021). Conductive PEDOT:PSS-based organic/inorganic flexible thermoelectric films and power generators. *Polymers*, 13(2), 210. doi: 10.3390/polym13020210

Peil, A., Zhan, P. & Liu, N. (2020). DNA origami catenanes templated by gold nanoparticles. *Small*, 16(6), 1905987. doi: https://doi.org/10.1002/smll.201905987

Pruneanu, S., Al-Said, S., Dong, L., Hollis, T., Galindo, M., Wright, N., Houlton, A. & Horrocks, B. R.(2008). Self-assembly of DNA-templated polypyrrole nanowires: spontaneous formation of conductive nano ropes. *Advanced Functional Materials*, 18(16), 2444-2454. doi: 10.1002/adfm.200701336

Sharifi-Viand, A., Mahjani, M., Moshrefi, R. & Jafarian, M. (2015). Diffusion through the self-affine surface of polypyrrole film. *Vacuum*, 114, 17-20. doi: 10.1016/j.vacuum.2014.12.030

Soler Besumbes, E., Fornaguera, C., Monge, M., García-Celma, M., Carrión, J., Solans, C. & Dols-Perez, A. (2019). PLGA cationic nanoparticles, obtained from nano-emulsion templating, as potential DNA vaccines. *European Polymer Journal*, 120, 109229. doi: 10.1016/j.eurpolymj.2019.109229

Stejskal, J. & Prokeš, J. (2020). Conductivity and morphology of polyaniline and polypyrrole prepared in the presence of organic dyes. *Synthetic Metals*, 264, 116373. doi: 10.1016/j.synthmet.2020.116373

Wadatkar, N. & Waghuley, S. (2019). Transport studies on one-pot chemically synthesized conducting polyindole in aqueous solution. *Frontier Research Today*, 2, 2001. doi: https://doi.org/10.31716/frt.201902001

Wang, S., Meng, W., Lv, H., Wang, Z. & Pu, J. (2021). Thermal insulating, light-weight and conductive cellulose/aramid nanofibers composite aerogel for pressure sensing. *Carbohydrate Polymers*, 270, 118414. doi: 10.1016/j.carbpol.2021.118414

Watson, S., Hedley, J., Galindo, M., Al-Said, S., Wright, N., Connolly, B. & Horrocks, B. R. & Houlton, A. (2012). Synthesis, characterisation and electrical properties of supramolecular DNA-templated polymer nanowires of 2,5-(bis-2-thienyl)-pyrrole. *Chemistry - A European Journal*, 18(38), 12008-12019. doi: 10.1002/chem.201201495

Watson, S., Mohamed, H., Horrocks, B. & Houlton, A. (2013). Electrically conductive magnetic nanowires using an electrochemical DNA-templating route. *Nanoscale*, 5(12), 5349. doi: 10.1039/c3nr00716b

Watson, S., Pike, A., Pate, J., Houlton, A. & Horrocks, B. (2014). DNA-templated nanowires: morphology and electrical conductivity. *Nanoscale*, 6(8), 4027-4037. doi: https://doi.org/10.1039/c3nr06767j

Wei, Y., Liu, M., Han, W., Li, G., Hao, C. & Lei, Q. (2019). Charge injection characteristics of semi-conductive composites with carbon black-polymer for HVDC cable. *Polymers*, 11(7), 1134. doi: 10.3390/polym11071134

Yahaya, M. (2020a). Spectroscopic, microscopic and electrical characterization of nanoscopic polyindole DNA-templated nanomaterials. *IOP Conference Series: Materials Science and Engineering*, 805(1), 012007. doi: 10.1088/1757-899x/805/1/012007

Yahaya, M. (2020b). Synthesis and characterization of nanostructured DNA-templated polyimidazole nanowire. *IOP Conference Series: Materials Science and Engineering*, 805(1), 012008. doi: 10.1088/1757-899x/805/1/012008

Yamada, H. & Kobayashi, K. (2019). SS2-2 Frontiers of AFM imaging method –high-resolution AFM in liquids and subsurface imaging–. *Microscopy*, 68(Supp), i28-i28. doi: 10.1093/jmicro/dfz067

Yamaguchi, I., Tariqul, I. & Wang, A. (2021). Conjugated polymers with anionic dyes: Synthesis, properties, and sensing ability for nucleosides, DNA, and BSA. *Journal of Applied Polymer Science*, 138(33), 50810. doi: 10.1002/app.50810